Strojniški vestnik - Journal of Mechanical Engineering 62(2016)9, 511-520

DOI:10.5545/sv-jme.2016.3188 Original Scientific Paper
Received for review: 2015-11-11
Received revised form: 2016-03-30
Accepted for publication: 2016-05-16

Slip Flow of Nanofluids between Parallel Plates Heated with a Constant Heat Flux

Ayşegül Öztürk - Kamil Kahveci*
Trakya University, Turkey

This study investigates the steady fully developed laminar flow and heat transfer of nanofluids between parallel plates heated with a constant heat flux. The governing equations were solved analytically under the boundary conditions of slip velocity and temperature jump. Water was taken as the base fluid and Cu, CuO and Al_2O_3 as the nanoparticles. The results were obtained for the slip factor in the range of 0 to 0.04, for the Brinkman number in the range of –0.1 to 0.1, for three different values of the ratio of the liquid layering thickness to the particle radius (0.1, 0.2, and 0.4) and for the solid volume fraction ranging from 0 % to 8 %. The results show that the nanoparticle presence in the base fluid has a significant effect on both the velocity field and heat-transfer characteristics. The average Nusselt number increases considerably with the increase of the nanoparticle solid volume fraction. The average Nusselt number takes much higher values for high values of the ratio of the liquid layering thickness to the nanoparticle radius. The average heat transfer rate of nanofluids between parallel plates ranges from the highest to the lowest when Cu, Al_2O_3, and CuO are used as nanoparticles, respectively.
Keywords: slip flow, nanofluid, parallel plate, slip factor, Nusselt number

Highlights

- *The nanoparticle usage has a considerable effect on both the velocity field and heat transfer characteristics.*
- *Velocity takes lower values with the increase of the nanoparticle solid volume fraction.*
- *The average Nusselt number increases considerably with the increase of the nanoparticle volume fraction and ratio of the liquid layering thickness to the nanoparticle radius.*
- *The average Nusselt number from the highest to the lowest is for the nanofluids of Cu, Al_2O_3, and CuO nanoparticles.*
- *The average heat transfer rate shows a decrease with the increase of the Brinkman number.*
- *The average heat transfer rate gets higher values for the positive values of the Brinkman number and lower values for the high negative values of the Brinkman number as the slip factor increases.*

0 INTRODUCTION

Flow and heat transfer in microchannels have attracted the interest of many researchers due to several application areas such as the electronic industry, microfabrication technology, and biomedical engineering. In particular, one of the main issues of the electronic industry nowadays is the transfer of heat generated in state-of-the-art chips at a rate as high as possible **[1]**. Since traditional air cooling systems cannot meet the demand for an efficient cooling, novel methods are being developed and analysed **[1]**. Cooling of electronic equipment with liquid flow in microchannels is an effective method of heat removal, which has the advantage of high heat capacity and conductivity of the liquids and the large surface area to volume ratio of the microchannels **[2]** and **[3]**.

Fluid flow and heat transfer in microscale show differences from macroscale as the surface effects become more important at micro-scale flow. The major difference between macro- and micro-scale flows is slip velocity and temperature jump on the walls. For gas micro-scale flows, flow regimes can be slip ($0.001 < Kn < 0.1$), transient ($0.1 < Kn < 10$) and free molecular flow ($Kn > 10$). In contrast, for liquid micro-scale flows, the slip flow regime is primarily observed **[4]**. Liquid slip flow occurs when there is little interaction between the liquid and the solid surface, which occurs when liquids are non-wetting or when air (partly) covers the channel walls **[5]**. Both experimental and theoretical studies on liquid slip flow are available in the literature. Lichter et al. **[6]** studied the mechanisms for the liquid slip along the solid surfaces and observed that slip occurs by two different mechanisms: localized defect propagation and a concurrent slip of large domains. Their results also show that well-defined transitions between these mechanisms occur. Martini et al. **[7]** studied the molecular mechanisms of liquid slip. Their results indicate that global slip causes an increase in the number of slipping atoms, leading to an increase in the slip length. The slip length approaches a constant value when forcing has significantly large values. Guan et al. **[8]** performed an experimental and theoretical analysis of the slip flow in super-hydrophobic microtubes. Their results indicate that the decrease in the slip length and slip velocity with an increase in the pressure and Reynolds number is the dominant factor

*Corr. Author's Address: Trakya University, Mechanical Engineering Department, 22180 Edirne, Turkey, kamilk@trakya.edu.tr

in the total resistance reduction in microtubes. Yu et al. [9] experimentally investigated slip flow in super-hydrophobic microtubes and concluded that the slip length shows a dependency on the Reynolds number similar to the pressure drop reduction. Lee et al. [10] investigated slip on a nanostructured surface and found that the liquid slip shows an increase with a decrease of the characteristic length, and it is more pronounced when the nonlinearity increases. Malvandi and Ganji [11] performed a theoretical study on the convective heat transfer of nanofluids in a circular microchannel under the effect of a uniform magnetic field. Their results show that the velocity gradients near the solid surface increases when the magnetic field is present. Therefore, slip velocity increases, and an increase is seen in the heat transfer rate and pressure drop. Nikkah et al. [12] investigated the slip flow of nanofluids in a microchannel with an oscillating heat flux and concluded that the Nusselt number experiences an increase when the slip coefficient has higher values. The increase in the Nusselt number has higher values for high values of the Reynolds number.

Another factor important in microscale flows is viscous dissipation. Resulting from high shear stress, viscous dissipation acts as a heat source and therefore influences temperature field severely.

There are a number of studies in the literature on liquid flow and heat transfer in microchannels. Xu et al. [13] investigated the liquid flow in microchannels and found that the viscous dissipation influences temperature, pressure, and velocity distributions significantly. Satapathy [14] studied steady-state heat transfer and fluid flow in an infinite microtube and found that at the fully-developed conditions the Nusselt number shows a decrease with an increase in the slip factor. Ngoma and Erchiqui [15] investigated liquid slip flow between two parallel plates with an imposed heat flux. The results show that the Nusselt number increases when the dimensionless slip coefficient increases. Celata et al. [16] studied forced convection heat transfer in microtubes and observed that a decrease is seen in the Nusselt number with a decrease in the diameter. Garcia-Hernando et al. [17] performed an experimental study on liquid flow in a micro-heat exchanger. The results show that the thickness and material of the plate are two important factors in micro-heat exchanger design. Peng and Peterson [18] studied convective heat transfer and fluid flow of water in microstructures and found that the Nusselt number shows a dependency on the Reynolds number, the Prandtl number, the microchannel aspect ratio, and the ratio between the hydraulic diameter and the microchannel width. They also found that geometrical configuration of microchannel has a critical effect on heat transfer. Yang et al. [19] studied the influence of interfacial electrokinetic phenomena on liquid flow and heat transfer in rectangular microchannels and concluded that flow and heat transfer are considerably affected by the presence of the electric double layer and the induced electrokinetic flow. Asthana et al. [1] investigated the segmented flow of two immiscible liquids in a microchannel experimentally and found that the Nusselt number increases up to four times in the segmented flow as compared to the pure water flow. Liu et al. [20] conducted an experimental study on liquid flow and heat transfer in a rectangular microchannel with longitudinal vortex generators. They found that the heat transfer performance improves 9 % to 21 % for laminar flow and 39 % to 90 % for turbulent flow, while the pressure drop increases 34 % to 83 % for laminar flow and 61 % to 169 % for turbulent flow. Liu et al. [21] performed a numerical study on the heat transfer performance of microchannels with different surface microstructures. The results show that the shield-shaped groove microchannel has the highest heat exchange performance.

From the literature given above, it can be concluded that heat transfer enhancement methods for liquid flow in microchannels have been investigated extensively in recent years. As is well known, one of the heat transfer enhancement methods is to use nanoparticles within a base fluid. The addition of nanoparticles to a base fluid results in an anomalous increase in the effective thermal conductivity of the fluid. There is only a limited number of studies in the literature investigating the effects of nanoparticle usage on flow and heat transfer in microchannels. Koo and Kleinstreuer [22] studied the steady laminar flow of nanofluids in microchannels. The results show that nanoparticles of high thermal conductivity and channels with high aspect ratios are advantageous. Raisi et al. [23] made a numerical investigation on the laminar forced convection of nanofluids in a microchannel and found that the average Nusselt number is considerably influenced by nanofluid solid volume fraction and slip velocity coefficient for high Reynolds numbers. Jung et al. [24] conducted an experimental investigation on the forced convective heat transfer of water-based Al_2O_3 nanofluids in microchannels. Their results show that the convective heat transfer coefficient in a laminar flow regime increases up to 32 % as compared to the pure water at a volume fraction of 1.8 % without a considerable friction loss.

The aim of this study is to perform and analytical investigation on the slip flow of nanofluids between two parallel plates heated with a constant heat flux. The results were analysed to reveal the effects of solid volume fraction and the ratio of the liquid layering thickness to the nanoparticle radius on the flow and heat transfer.

1 METHODS

The geometry and the coordinate system used to investigate the slip flow and heat transfer of nanofluids between parallel plates heated with a constant heat flux are shown in Fig. 1. The fluid flow was assumed to be steady, laminar, incompressible and fully developed with constant thermo-physical properties. The nanofluid was assumed to be a single phase fluid as the solid nanoparticles are of a very small size and are easily fluidized. In the single phase approach, fluid and solid particles are assumed to be in thermal equilibrium and move with the same velocity [25]. The coordinate system is at the centre of the microchannel. The *x*-axis was taken along the centreline of the microchannel, and the *y*-axis was taken normal to it. Under these conditions, the governing equations including the viscous dissipation take the following form:

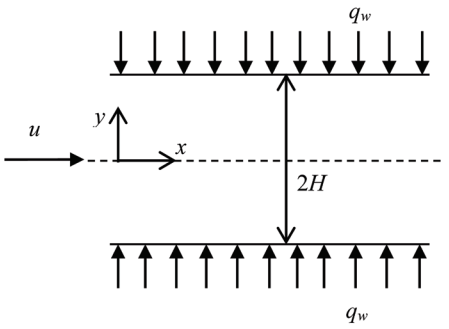

Fig. 1. *Geometry and the coordinate system*

$$\frac{d^2u}{dy^2} = \frac{1}{\mu_{nf}}\frac{dp}{dx}, \tag{1}$$

$$u\frac{\partial T}{\partial x} = \alpha_{nf}\frac{\partial^2 T}{\partial y^2} + \frac{\mu_{nf}}{\left(\rho c_p\right)_{nf}}\left(\frac{du}{dy}\right)^2, \tag{2}$$

where u is the dimensional velocity component in the x direction, p is the dimensional pressure, and T is the temperature. μ is the viscosity, ρc_p is the heat capacity and α is the thermal diffusivity.

As can be seen from Eqs. (1) and (2), flow and heat transfer has only a one-way coupling by the velocity term in the energy equation. This is because the buoyancy forces are negligible, and the thermophysical properties of the fluid were assumed to be constant [26]. The Grashof number, representing the importance of buoyancy forces, is extremely low for this flow regime and configuration as the flow is pressure driven and the Grashof number is proportional to the 3rd power of the characteristic length $[(2h)^3]$. The term $(2h)^3$ has extremely low values for a microchannel.

The viscosity of the nanofluid was estimated in this study using the following model proposed by Brinkman for a two-phase mixture [27]:

$$\mu_{nf} = \frac{\mu_f}{\left(1-\phi\right)^{2.5}}, \tag{3}$$

where ϕ is the solid volume fraction of the nanoparticles. It is useful to express that the experimental results of Xuan et al. [28] for the effective viscosity of the transformer oil-water nanofluid and of the water-copper nanofluid in the temperature range of 20 °C to 50 °C show reasonably good agreement with the Brinkman model.

The thermal diffusivity of nanofluids is defined as following:

$$\alpha_{nf} = \frac{k_{nf}}{\left(\rho c_p\right)_{nf}}, \tag{4}$$

where k is the thermal conductivity.

The reason behind the noticeable heat transfer characteristics of nanofluids is the thermal conductivity, and it is a function of the thermal conductivity of both the base fluid and nanoparticle, as well as the volume fraction, the surface area, the shape of the nanoparticles, and distribution of dispersed particles [25]. Due to the lack of a theoretical formula in the literature for the calculation of thermal conductivity of nanofluids, models for the solid-liquid suspensions with relatively large particles are generally used to estimate it. One model of this type was developed by Yu and Choi [29]. In this model, nanofluid is assumed to consist of a bulk liquid, solid nanoparticles, and solid-like nanolayers (see Fig. 2) acting as a thermal bridge between a solid nanoparticle and a bulk liquid. With the assumption of $k_{layer} = k_s$, the model for spherical nanoparticles takes the following form:

$$\frac{k_{nf}}{k_f} = \frac{k_s + 2k_f + 2\left(k_s - k_f\right)\left(1+\right)^3\varphi}{k_s + 2k_f - \left(k_s - k_f\right)\left(1+\right)^3\varphi}, \tag{5}$$

where β is the ratio of the liquid layering thickness to the nanoparticle radius. To validate their model, Yu and Choi [29] made a comparison between their model results for β = 0.1 and experimental results in the literature and found an acceptable agreement. They observed that the model is more effective for the nanofluids with nanoparticles of less than 10 nm diameter. This model was used in the present study to estimate the effective thermal conductivity of nanofluids.

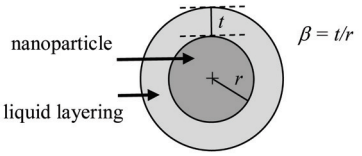

Fig. 2. *Liquid layering around a nanoparticle*

The heat capacity of nanofluids is defined as [16]:

$$\left(\rho c_p\right)_{nf} = \left(1-\phi\right)\left(\rho c_p\right)_f + \phi\left(\rho c_p\right)_s. \tag{6}$$

If the wall is not moving, the velocity-slip and the temperature-jump boundary conditions can be defined as [4]:

$$u_s = \pm\delta \left.\frac{\partial u}{\partial y}\right|_w, \quad T_s - T_w = \pm\frac{\delta}{Pr}\left.\frac{\partial T}{\partial y}\right|_w, \tag{7}$$

where u_s is the slip velocity, δ the slip factor, T_s the temperature of the base fluid at the wall, T_w the wall temperature.

1.1 Velocity Profile

The dimensionless variables can be defined as:

$$X = \frac{x}{H}, \quad Y = \frac{y}{H}, \quad U = \frac{u}{u_{m,f}},$$
$$U_s = \frac{u_s}{u_{m,f}}, \quad \Delta = \frac{\delta}{2H}, \quad P = \frac{pH}{\mu_f u_{m,f}}, \tag{8}$$

where $u_{m,f}$ is the mean velocity of the base fluid and is defined as:

$$u_{m,f} = \frac{1}{2H}\int_{-H}^{H} u dy. \tag{9}$$

The dimensionless x-momentum equation and associated boundary conditions for hydrodynamically fully developed flow can then be obtained as:

$$\frac{d^2U}{\partial Y^2} = \frac{\mu_f}{\mu_{nf}}\frac{dP}{dX}, \tag{10}$$

$$\left.\frac{dU}{dY}\right|_{Y=0} = 0 \quad at \quad Y = 0, \tag{11}$$

$$U = U_s = -2\Delta\left.\frac{dU}{dY}\right|_{Y=1} \quad at\ Y = 1. \tag{12}$$

The analytical solution of Eq. (10) subjected to the boundary conditions given in Eqs. (11) and (12) is:

$$U = \frac{3}{2}\frac{\mu_f}{\mu_{nf}}\left[\frac{1-Y^2+4\Delta}{1+6\Delta}\right]. \tag{13}$$

1.2 Temperature Distribution

The dimensionless temperature can be defined as:

$$\theta\left(Y\right) = \frac{T-T_s}{\frac{q_w H}{k_f}}. \tag{14}$$

The dimensionless energy equation can then be obtained as:

$$\frac{\partial^2\theta}{\partial Y^2} = \frac{k_f}{k_{nf}}\left[\frac{\left(\rho c_p\right)_{nf}}{\left(\rho c_p\right)_f} aU - \frac{\mu_{nf}}{\mu_f} Br\left(\frac{dU}{dY}\right)^2\right], \tag{15}$$

where $a = \frac{Hu_{m,f}\left(\rho c_p\right)_f}{q_w}\frac{dT_s}{dx}$ and Br is the modified Brinkman number defined as:

$$Br = \frac{\mu_f u_{m,f}^2}{q_w H}. \tag{16}$$

The energy equation is subjected to the following boundary conditions:

$$\left.\frac{d\theta}{dY}\right|_{Y=0} = 0 \quad at \quad Y = 0, \tag{17}$$

$$\theta = 0, \quad \left.\frac{d\theta}{dY}\right|_{Y=1} = \frac{k_f}{k_{nf}} \quad at \quad Y = 1. \tag{18}$$

The solution of Eq. (15) under the thermal boundary conditions given in Eqs. (17) and (18) is:

$$\theta\left(Y\right) = \frac{T-T_s}{\frac{q_w H}{k_f}} = \frac{k_f}{k_{nf}}\left\{\left[\frac{\mu_f}{\mu_{nf}}\frac{3Br}{\left(1+6\Delta\right)^3} + \frac{1}{1+6\Delta}\right]\times\right.$$
$$\times\left[-\frac{1}{8}Y^4 + \frac{3}{4}Y^2 + 3\Delta\left(Y^2-1\right) - \frac{5}{8}\right] -$$
$$\left. -\frac{\mu_f}{\mu_{nf}}\frac{3Br}{4\left(1+6\Delta\right)^2}\left[Y^4-1\right]\right\}. \tag{19}$$

Eq. (19) is in terms of T_s and can be transformed into an equation in terms of T_w using the following conversion formula:

$$\frac{T_s - T_w}{\frac{q_w H}{k_f}} = -2\frac{k_f}{k_{nf}}\frac{\Delta}{Pr}. \tag{20}$$

Therefore, Eq. (19) takes the following form:

$$\tilde{\theta} = \frac{T - T_w}{\frac{q_w H}{k_f}} = \frac{k_f}{k_{nf}}\left\{\left[\frac{\mu_f}{\mu_{nf}}\frac{3Br}{(1+6\Delta)^3} + \frac{1}{1+6\Delta}\right]\times \right.$$
$$\times\left[-\frac{1}{8}Y^4 + \frac{3}{4}Y^2 + 3\Delta\left(Y^2 - 1\right) - \frac{5}{8}\right] -$$
$$\left. -\frac{\mu_f}{\mu_{nf}}\frac{3Br}{4(1+6\Delta)^2}\left[Y^4 - 1\right] - 2\frac{\Delta}{Pr}\right\}. \tag{21}$$

For fully developed flows, the mean fluid temperature is preferred in defining the Nusselt number instead of the centreline temperature. The mean temperature of the fluid is defined as:

$$\tilde{\theta}_{m,nf} = \frac{T_{m,nf} - T_w}{\frac{q_w H}{k_f}} =$$
$$= \frac{k_f}{k_{nf}}\left\{-\frac{1}{35}\left[\frac{\mu_f}{\mu_{nf}}\frac{3Br}{(1+6\Delta)^4} + \frac{1}{(1+6\Delta)^2}\right]\times \right.$$
$$\times\left[420\Delta^2 + 168\Delta + 17\right] +$$
$$\left. \boxplus\frac{\mu_f}{\mu_{nf}}\frac{6Br}{35(1+6\Delta)^3}\left[21\Delta + 4\right] - 2\frac{\Delta}{Pr}\right\}. \tag{22}$$

The dimensionless mean temperature in term of the modified Brinkman number can then be obtained as:

$$\tilde{\theta}_{m,nf} = \frac{T_{m,nf} - T_w}{\frac{q_w H}{k_f}} =$$
$$= \frac{k_f}{k_{nf}}\left\{-\frac{1}{35}\left[\frac{\mu_f}{\mu_{nf}}\frac{3Br}{(1+6\Delta)^4} + \frac{1}{(1+6\Delta)^2}\right]\times \right.$$
$$\times\left[420\Delta^2 + 168\Delta + 17\right] +$$
$$\left. + \frac{\mu_f}{\mu_{nf}}\frac{6Br}{35(1+6\Delta)^3}\left[21\Delta + 4\right] - 2\frac{\Delta}{Pr}\right\}. \tag{23}$$

The convective heat transfer coefficient can be defined as:

$$h_{nf} = \frac{q_w}{T_w - T_{m,nf}}. \tag{24}$$

Therefore, the average Nusselt number takes the following form:

$$Nu = -\frac{2}{\tilde{\theta}_{m,nf}}. \tag{25}$$

After the necessary substitution, the average Nusselt number becomes:

$$Nu = -2\left\{\frac{k_f}{k_{nf}}\left\{-\frac{1}{35}\left[\frac{\mu_f}{\mu_{nf}}\frac{3Br}{(1+6\Delta)^4} + \frac{1}{(1+6\Delta)^2}\right]\times \right.\right.$$
$$\times\left[420\Delta^2 + 168\Delta + 17\right] +$$
$$\left.\left. + \frac{\mu_f}{\mu_{nf}}\frac{6Br}{35(1+6\Delta)^3}\left[21\Delta + 4\right] - 2\frac{\Delta}{Pr}\right\}\right\}^{-1}. \tag{26}$$

2 RESULTS AND DISCUSSION

Hydrodynamically and thermally fully developed slip flow of nanofluids between parallel plates heated with a constant heat flux was investigated in this study. Water was taken as the working fluid with $Pr = 6.2$ and Cu, CuO, and Al_2O_3 as the nanoparticles. The thermo-physical properties of the base fluid and nanoparticles are shown in Table 1. The results were obtained for the slip factor ranging from 0 to 0.04, for the Brinkman number ranging from –0.1 to 0.1 and for the solid volume fraction ranging from 0 % to 8 %, and for the ratio of the liquid layering thickness to the nanoparticle radius ranging from 0 to 0.4.

To validate the analysis, the results obtained for air as the heat transfer fluid were compared with the results of the studies available in the literature. The comparison shows that there is a good agreement between the results (see **[30]**).

Table 1. *Thermo-physical properties of the base fluid and nanoparticles*

Property	Water	Cu	CuO	Al_2O_3
ρ [kg/m³]	997.1	8933	6500	3970
c_p [J/(kgK)]	4179	385	535.6	765
k [W/(mK)]	0.613	400	20	40

The dimensionless axial velocity profile is shown in Fig. 3 for various values of the slip factor and solid volume fraction. As the slip factor increases, slip velocity on the walls increases and velocity in

the core region takes lower values. Higher slip is associated with the lower core velocities as expected. As it is seen in Fig. 3, velocity gets lower values with an increase in the nanoparticle solid volume fraction. As Eq. (3) suggests, an increase in the nanoparticle volume fraction causes an increase in the viscosity of the nanofluid. Therefore, viscose forces get higher values and a decrease in velocity is observed as the nanoparticle volume fraction is increased.

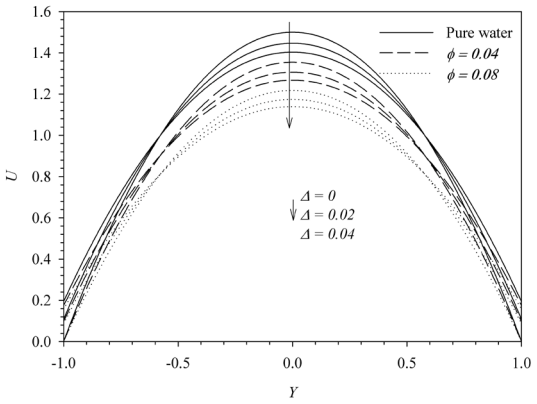

Fig. 3. *Velocity profiles for various values of the slip factor and solid volume fraction*

Variation of the average Nusselt number with the slip factor is seen in Figs. 4 to 6 for various values of the Brinkman number, solid volume fraction, and the ratio of liquid layering thickness to nanoparticle radius. The positive values of the Brinkman number mean that the fluid is being heated by the hot wall, while the negative values mean that the fluid is being cooled by the cold wall. As the slip factor increases, temperature jump at the microchannel walls increases. This has a negative effect on the heat transfer. However, an increase in the slip factor also decreases the viscous forces near the wall. This has a positive effect on the convective heat transfer from the wall to the fluid and a negative effect on the convective heat transfer from the fluid to the wall when the viscous dissipation is at significant levels. As a result of the combined effect of the velocity and temperature jumps, an increase is seen in the heat transfer for the positive values of the Brinkman number and a decrease in the high negative values of the Brinkman number. As it can be seen from Figs. 4 to 6, the effect of the slip factor on the heat transfer decreases when the Brinkman number has lower values. For the hot wall case, viscous dissipation decreases the temperature difference between the solid surface and the fluid. Therefore, the average Nusselt number takes lower values with an increase in the Brinkman

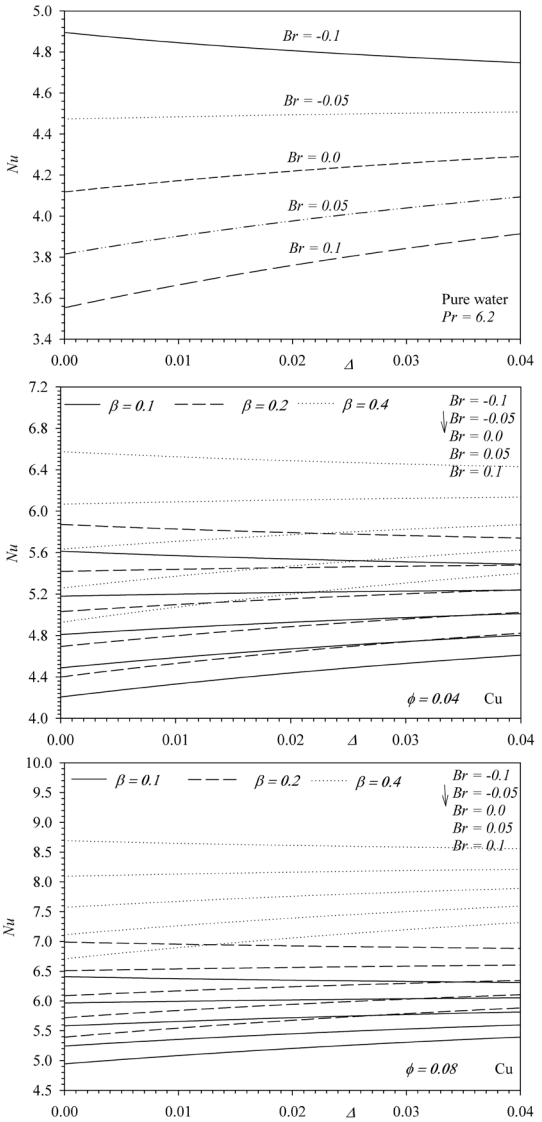

Fig. 4. *Variation of the average Nu number with the slip factor for the Cu nanofluid*

number. For the cold wall case, viscous dissipation causes an increase in the temperature difference between the solid surface and fluid. Therefore, the average Nusselt number increases with an increase in the Brinkman number in the negative direction. As seen from Figs. 4 to 6, the nanoparticle usage has a significant effect on the average heat transfer rate, and the average Nusselt number increases considerably with the increase of the nanoparticle volume fraction. As was observed before, velocity decreases with the increase of the nanoparticle volume fraction. This creates a negative effect on heat transfer. Despite this negative effect, the average Nusselt number increases

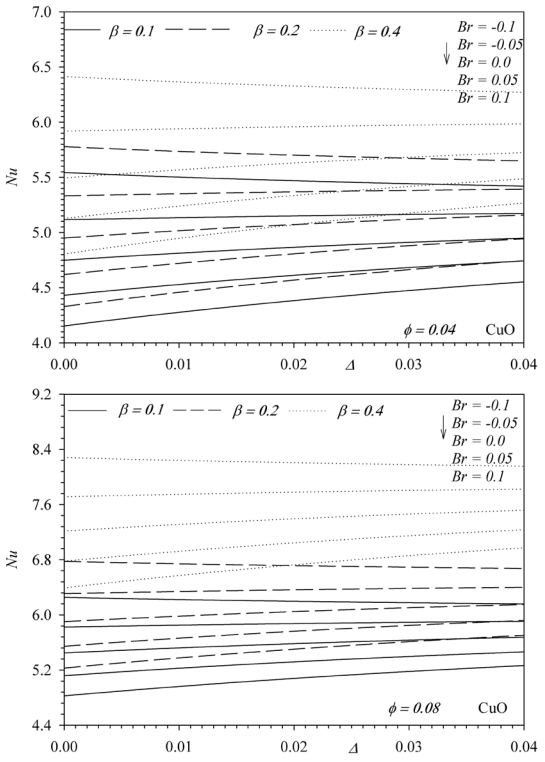

Fig. 5. *Variation of the average Nu number with the slip factor for the CuO nanofluid*

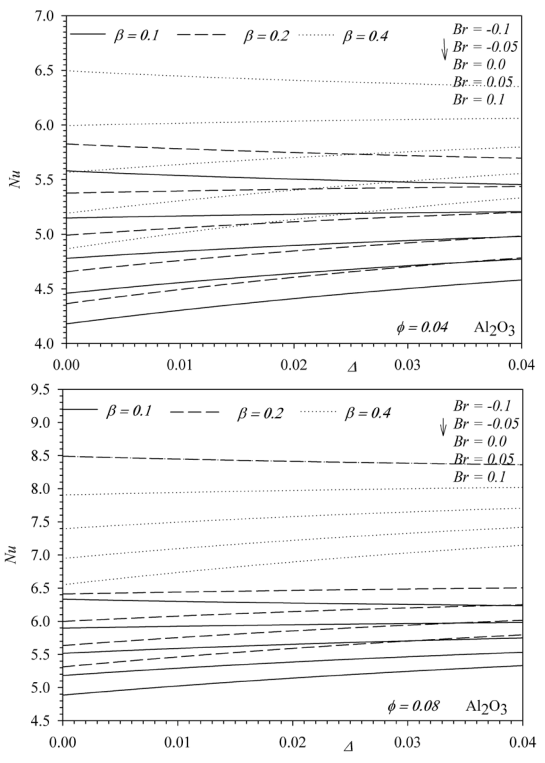

Fig. 6. *Variation of the average Nu number with the slip factor for the Al_2O_3 nanofluid*

with the increase of the nanoparticle volume fraction as the energy transport between the wall and fluid increases considerably as a result of the increase in the thermal conductivity of the fluid. The effect of the slip factor on heat transfer decreases with an increase in the nanoparticle volume fraction as the thermal diffusion has higher values. The average Nusselt number has much higher values for the higher values of the ratio of the liquid layering thickness to the nanoparticle radius, or in other words for lower values of the nanoparticle diameter. As expected, the average Nusselt number for the nanoparticles with a

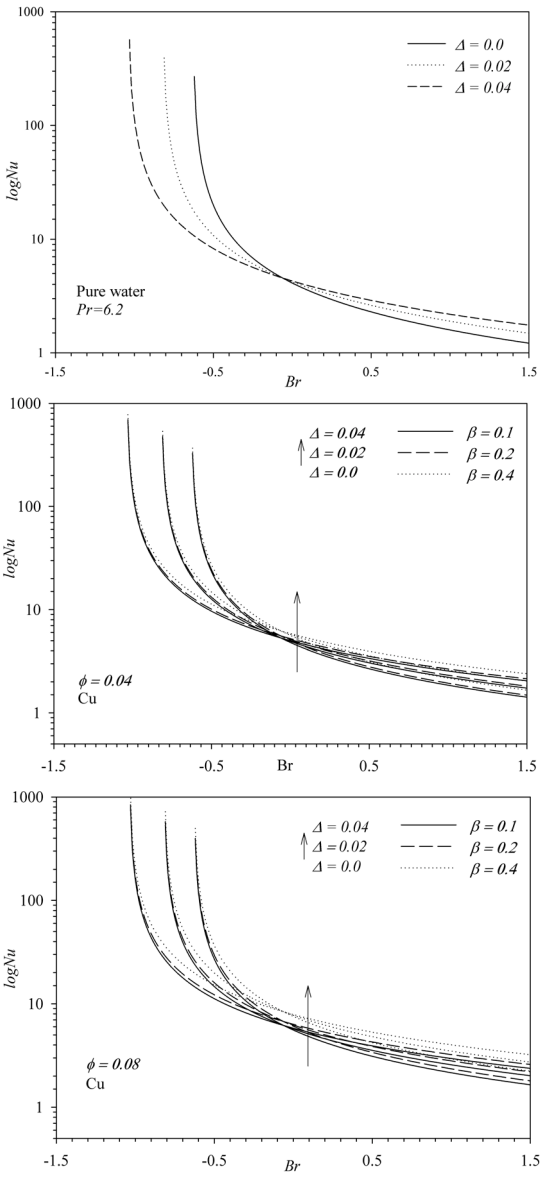

Fig. 7. *Variation of the average Nu number with the Br number for the Cu nanofluid*

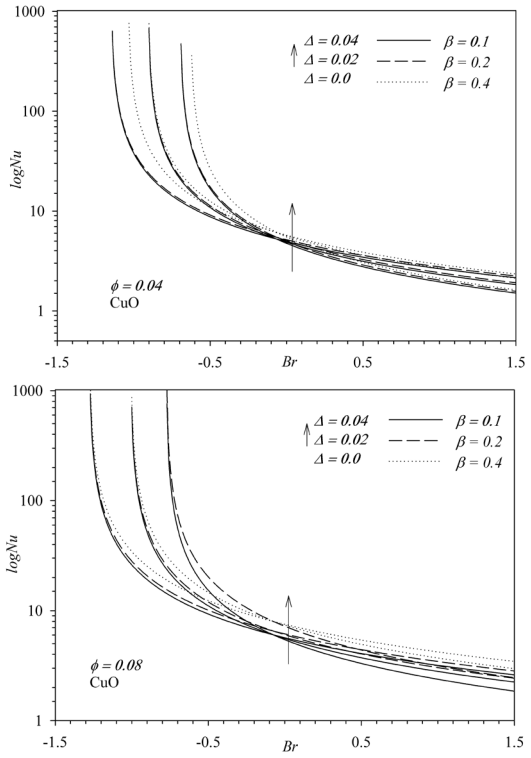

Fig. 8. *Variation of the average Nu number with the Br number for the CuO nanofluid*

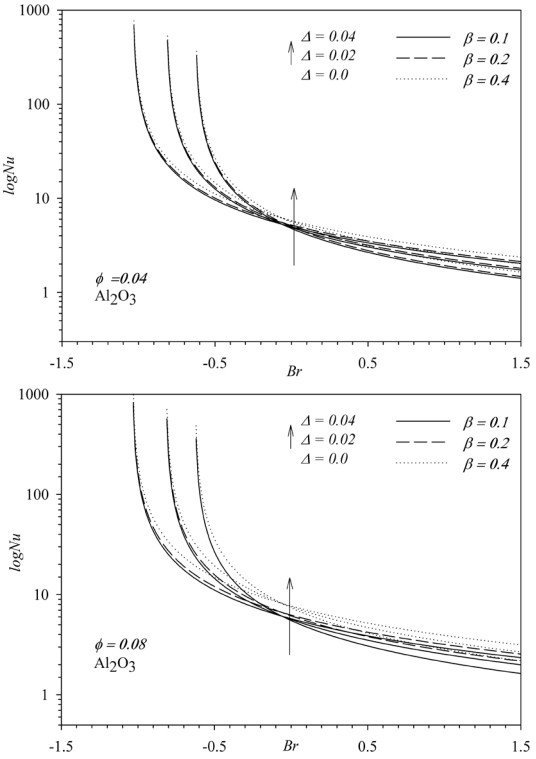

Fig. 9. *Variation of the average Nu number with the Br number for the Al_2O_3 nanofluid*

higher thermal conductivity has higher values. It is the highest for Cu nanoparticles and the lowest for CuO nanoparticles.

The variation of the average Nusselt number with the Brinkman number is seen in Figs. 7 to 9 for various values of the slip factor, solid volume fraction and ratio of the liquid layering thickness to the nanoparticle radius. As it can be observed from the figures, the average heat transfer rate shows a steep decrease first and then progressively approaches to an asymptotic value with the increase of the Brinkman number. As can also be seen from the figures, the average Nusselt number shows a similar trend for all the nanofluids considered in this study. Only a magnitude difference is seen in the average Nusselt number for different nanofluids. As stated before, this can be attributed to the more effective thermal energy transport between the wall and the nanofluid.

3 CONCLUSIONS

The slip flow of nanofluids between two parallel plates heated with a constant heat flux was investigated in this study. Water was taken as the base fluid and Cu, CuO, and Al_2O_3 as the nanoparticles. The concluding remarks are:

- The nanoparticle usage has a significant effect on both the velocity field and the heat transfer characteristics.
- The average heat transfer rate increases considerably as the nanoparticle solid volume fraction is increased.
- The average Nusselt number takes much higher values for the high values of the ratio of the liquid layering thickness to the nanoparticle radius.
- The average heat transfer rate of nanofluids ranges from the highest to the lowest, when Cu, Al_2O_3, and CuO nanoparticles are used, respectively.

4 NOMENCLATURES

Br	modified Brinkman number
c_p	specific heat at constant pressure [J/(kgK)]
h	convective heat transfer coefficient [W/(m²K)]
H	half distance between plates [m]
Kn	Knudsen number
k	thermal conductivity [W/(mK)]
Nu	Nusselt number
p	pressure [Pa]
Pr	Prandtl number
q_w	wall heat flux [W/m²]
T	temperature [K]

u velocity component in the x direction [m/s]
U dimensionless velocity
x dimensional axial coordinate [m]
X dimensionless axial coordinate
y dimensional normal coordinate [m]
Y dimensionless normal coordinate

Greek Symbols
α thermal diffusivity [m²/s]
β ratio of the liquid layering thickness to the nanoparticle radius
δ slip factor [m]
Δ dimensionless slip factor
θ dimensionless temperature
$\tilde{\theta}$ dimensionless temperature
μ dynamic viscosity [Pas]
ρ density [kg/m³]
ϕ solid volume fraction

Subscripts
c centreline
f base fluid
layer solid-like nanolayer
m mean
nf nanofluid
s solid nanoparticles or slip
w wall

5 REFERENCES

[1] Asthana, A., Zinovik, I., Weinmueller, C., Poulikakos, D. (2011). Significant Nusselt number increase in microchannels with a segmented flow of two immiscible liquids: An experimental study. *International Journal of Heat and Mass Transfer*, vol. 54, no. 7-8, p. 1456–1464, **DOI:10.1016/j.ijheatmasstransfer.2010.11.048**.

[2] Tuckerman, D.B., Pease, R.F.W. (1981). High-performance heat sinking for VLSI. *IEEE Electron Device Letters*, vol. 2, no. 5, p. 126-129, **DOI:10.1109/EDL.1981.25367**.

[3] Upadhye, H.R., Kandlikar, S.G. (2004). Optimization of microchannel geometry for direct chip cooling using single phase heat transfer. *Proceedings of the 2nd International Conference on Microchannel and Minichannels*, p. 679-685, **DOI:10.1115/ICMM2004-2398**.

[4] Karimipour, A., Nezhad, A.H., D'orazio, A., Esfe, M.H., Safaei, M.R., Shirani, E. (2015). Simulation of copper-water nanofluid in a microchannel in slip flow regime using the lattice Boltzmann method. *European Journal of Mechanics - B/Fluids*, vol. 49, p. 89-99, **DOI:10.1016/j.euromechflu.2014.08.004**.

[5] Eijkel, J. (2007). Liquid slip in micro- and nanofluidics: recent research and its possible implications. *Lab on a Chip*, vol. 7, no. 3, p. 299-301, **DOI:10.1039/B700364C**.

[6] Lee, D.J.,Cho, K.Y., Jang, S., Song, Y.S., Youn, J.R. (2012). Liquid slip on a nanostructured surface. *Langmuir*, vol. 28, no. 28, p. 10488-10494, **DOI:10.1021/la302264t**.

[7] Martini, A., Roxin, A., Snurr, R.O., Wang, O., Lichter, S. (2008). Molecular mechanisms of liquid slip. *Journal of Fluid Mechanics*, vol. 600, p. 257-269, **DOI:10.1017/S0022112008000475**.

[8] Lichter, S., Roxin, A., Mandre, S. (2004). Mechanisms for liquid slip at solid surfaces. *Physical Review Letters*, vol. 93, no. 8, 086001, **DOI:10.1103/PhysRevLett.93.086001**.

[9] Malvandi, A., Ganji, D.D. (2014). Brownian motion and themophoresis effects on slip flow of alumina/water nanofluid inside a circular microchannel in the presence of a magnetic field. *International Journal of Thermal Sciences*, vol. 84, p. 196-206, **DOI:10.1016/j.ijthermalsci.2014.05.013**.

[10] Nikkhah, Z., Karimipour, A., Safaei, M.R., Forghani-Therani, P., Goodarzi, M., Dahari, M., Wongwises, S. (2015). Forced convective heat transfer of water/functionalized multi-walled carbon nanotube nanofluids in a microchannel with oscillating heat flux and slip boundary condition. *International Communications in Heat and Mass Transfer*, vol. 68, p. 69-77, **DOI:10.1016/j.icheatmasstransfer.2015.08.008**.

[11] Guan, N., Liu, Z., Jiang, G., Zhang, C., Ding, N. (2015). Experimental and theoretical investigations on the flow resistance reduction and slip flow in super-hydrophobic micro tubes. *Experimental Thermal and Fluid Science*, vol. 69, p. 45-57, **DOI:10.1016/j.icheatmasstransfer.2015.08.008**.

[12] Yu, Z., Liu, X., Kuang, G. (2015). Water slip flow in superhydrophobic microtubes within laminar flow region. *Chinese Journal of Chemical Engineering*, vol. 23, no. 5, p. 763-768, **DOI:10.1016/j.cjche.2014.12.010**.

[13] Xu, B., Ooi, K.T., Mavriplis, C., Zaghloul, M.E. (2002). Viscous dissipation effects for liquid flow in microchannels. *International Conference on Modeling and Simulation of Microsystems*, p. 100-103.

[14] Satapathy, A.K. (2010). Slip flow heat transfer in an infinite microtube with axial conduction. *International Journal of Thermal Sciences*, vol. 49, no. 1, p. 153-160, **DOI:10.1016/j.ijthermalsci.2009.06.012**.

[15] Ngoma, G.D., Erchiqui, F. (2007). Heat flux and slip effects on liquid flow in a microchannel. *International Journal of Thermal Sciences*, vol. 46, no. 11, p. 1076-1083, **DOI:10.1016/j.ijthermalsci.2007.02.001**.

[16] Celata, G.P., Cumo, M., Marconi, V., McPhail, S.J., Zummo, G. (2006). Microtube liquid single-phase heat transfer in laminar flow. *International Journal of Heat and Mass Transfer*, vol. 49, no. 19-20, p. 3538–3546, **DOI:10.1016/j.ijheatmasstransfer.2006.03.004**.

[17] García-Hernando, N., Acosta-Iborra, A., Ruiz-Rivas, U., Izquierdo, M. (2009). Experimental investigation of fluid flow and heat transfer in a single-phase liquid flow micro-heat exchanger. *International Journal of Heat and Mass Transfer*, vol. 52, no. 23-24, p. 5433–5446, **DOI:10.1016/j.ijheatmasstransfer.2009.06.034**.

[18] Peng, X.F., Peterson, G.P. (1996). Convective heat transfer and flow friction for water flow in microchannel structures. *International Journal of Heat and Mass Transfer*, vol. 39, no. 12, p. 2599-2608, **DOI:10.1016/0017-9310(95)00327-4**.

[19] Yang, C., Li, D., Masliyah, J.B. (1998). Modeling forced liquid convection in rectangular microchannels with electrokinetic effects. International Journal of Heat and Mass Transfer,

vol. 41, no. 24, p. 4229-4249, **DOI:10.1016/S0017-9310(98)00125-2**.

[20] Liu, C,. Teng, J-T., Chu, J.-C., Chiu, Y.-L., Huang, S., Jin, S., Dang, T., Greif, R., Pan, H.-H. (2011). Experimental investigations on liquid flow and heat transfer in rectangular microchannel with longitudinal vortex generators. *International Journal of Heat and Mass Transfer*, vol. 54, no. 13-14, p. 3069-3080, **DOI:10.1016/j.ijheatmasstransfer.2011.02.030**.

[21] Liu, Y., Cui, J., Jiang, Y.X., Li, W.Z. (2011). A numerical study on heat transfer performance of microchannels with different surface microstructures. Applied Thermal Engineering, vol. 31, no. 5, p. 921-931, **DOI:10.1016/j.applthermaleng.2010.11.015**.

[22] Koo, J., Kleinstreuer, C. (2005). Laminar nanofluid flow in microheat-sinks. *International Journal of Heat and Mass Transfer*, vol. 48, no. 13, p. 2652–2661, **DOI:10.1016/j.ijheatmasstransfer.2005.01.029**.

[23] Raisi, A., Ghasemi, B., Aminossadati, S.M. (2011). A numerical study on the forced convection of laminar nanofluid in a microchannel with both slip and no-slip conditions. *Numerical Heat Transfer, Part A: Applications: International Journal of Computation and Methodology*, vol. 59, no. 2, p. 114-129, **DOI:10.1080/10407782.2011.540964**.

[24] Jung, J.-Y., Oh, H.-S., Kwak, H.-Y. (2009). Forced convective heat transfer of nanofluids in microchannels. *International Journal of Heat and Mass Transfer*, vol. 52, no. 1-2, p. 466-472, **DOI:10.1016/j.ijheatmasstransfer.2008.03.033**.

[25] Kahveci, K. (2010). Buoyancy driven heat transfer of nanofluids in a tilted enclosure *Journal of Heat Transfer*, vol. 132, no. 6, 062501, **DOI:10.1115/1.4000744**.

[26] Aydın, O., Avcı, M. (2007). Analysis of laminar heat transfer in micro-Poiseuille flow, *International Journal of Thermal Sciences*, vol. 46, no. 1, p. 30-37, **DOI:10.1016/j.ijthermalsci.2006.04.003**.

[27] Brinkman, H.C. (1952). The viscosity of concentrated suspensions and solutions. *The Journal of Chemical Physics*, vol. 20, p. 571-581, **DOI:10.1063/1.1700493**.

[28] Xuan, Y., Li, Q., Xuan, Y., Li, Q. (1999). *Experimental research on the viscosity of nanofluids*. Report of Nanjing University of Science and Technology, Nanjing.

[29] Yu, W., Choi, S.U.S. (2003). The role of interfacial layers in the enhanced thermal conductivity of nanofluids: a renovated Maxwell model. *Journal of Nanoparticle Research*, vol. 5, no. 1, p. 167-171, **DOI:10.1023/A:1024438603801**.

[30] Ozturk, A. (2012). MHD slip flow between parallel plates heated with a constant heat flux. *Journal of Thermal Science and Technology*, vol. 33, no. 1, p. 11-20.